Computers and Electronics in Agriculture 160 (2019) 144–152

Contents lists available at ScienceDirect

Computers and Electronics in Agriculture

journal homepage: www.elsevier.com/locate/compag

Original papers

Predicting kernel processing score of harvested and processed corn silage via image processing techniques

Jessica L. Drewry[a], Brian D. Luck[a,*], Rebecca M. Willett[b,1], Eduardo M.C. Rocha[a], Joshua D. Harmon[a,2]

[a] Department of Biological Systems Engineering, University of Wisconsin-Madison, 460 Henry Mall, Madison, WI 53706, United States
[b] Department of Electrical and Computer Engineering, University of Wisconsin-Madison, 1415 Engineering Drive, Madison, WI 53706, United States

ARTICLE INFO

Keywords:
Kernel processing
Kernel processing score
Forage
Image processing
Silage

ABSTRACT

An image processing algorithm was developed to characterize the size distribution of corn kernel particles from Whole Plant Corn Silage (WPCS). The algorithm determines particle cross sectional area and maximum inscribed circle diameter as well as cumulative undersize percent, dimensions of significance, and key characteristics of the distribution including mean particle size, skewness, and kurtosis. Kernel Possessing Score (KPS) was derived from the area-weighted cumulative undersize percent of 4.75 mm. Samples of WPCS harvested using self-propelled forage harvester with crop processing roll gap clearance of 1, 2, 3, and 4 mm were analyzed in their fresh, dry, and sieved states. Algorithm results were compared with the standard method of mechanical sieving and found to be well correlated $r(23) = 0.8$, $p < 0.001$. Additionally, analysis of particles before and after sieving indicated that sieving significantly increased KPS for 1 ($t(5) = 6.6$, $p = 0.001$), 2 ($t(5) = 4.2$, $p = 0.01$), and 3 ($t(5) = 3.5$, $p = 0.02$) mm samples. This algorithm has the potential to more accurately determine KPS in field compared to currently available methods, allowing for adjustment of kernel processing during harvest which will improve silage quality.

1. Introduction

Proper kernel processing of whole-plant corn silage (WPCS) directly effects feed quality and milk yield once fed to dairy cows (Johnson et al., 2003; Weiss & Wyatt, 2000). Crop processing rolls, installed on forage harvesters, are two counter-rotating grooved cylinders placed behind the cutterhead (Shinners et al., 2000) that provide compression and shearing of the material passing between them further reducing the particle size of the corn kernels in the chopped WPCS. Particle size reduction of the corn kernels in WPCS provides increased total digestible nutrients and greater in vitro dry matter disappearance (Ferraretto & Shaver, 2012; Weiss & Wyatt, 2000). Mertens (2005) outlined a corn silage fragmentation index, more commonly known as Kernel Processing Score (KPS). Results from this work showed that corn kernel particles retained on a 4.75 mm sieve are incompletely fermented in the rumen of the cow and digestion of these particles is insufficient. Conversely, particles that passed through the 4.75 mm sieve are readily digested by the cow without any additional chewing. KPS has since been utilized for assessing sufficient WPCS kernel processing. To arrive at the KPS, samples are placed in a sieve shaker that oscillates the screens in the horizontal plane and taps in the vertical direction. Multiple screens are used and aperture size ranges from 26.9 mm to 0.053 mm. The mass of material retained on the screens is then utilized to calculate the geometric mean length, standard deviation of the particles in the sample, and other characteristics of the particle distribution (ASABE, 2012). While an accurate assessment of particle size distribution can be gained from this method, it is impractical for in-field assessment during harvest.

Currently, producers send a sample of the chopped and processed corn silage to a laboratory for particle size and nutrient analysis. Results return after the crop has been harvested when no machine setting adjustments can be made. Lammers et al. (1996) developed a shaker-box that implemented two screens with opening diameters of 19 mm and 8 mm. A 1.4 L sample of freshly harvested WPCS was loaded into the device and manual shaking on a flat surface to generate the separation of materials. The percentage of the original sample retained by each screen, by mass, provided the assessment of particle size distribution of WPCS samples. Updates to this research (Kononoff et al., 2003) require

* Corresponding author.
E-mail addresses: bluck@wisc.edu (B.D. Luck), willett@uchicago.edu (R.M. Willett), Joshua.Harmon@cnhind.com (J.D. Harmon).
[1] Departments of Statistics and Computer Science, University of Chicago, 5747 S. Ellis Avenue, Chicago, IL 60637, United States.
[2] 500 Diller Avenue MS 640, New Holland, PA 17557, United States.

https://doi.org/10.1016/j.compag.2019.03.020
Received 9 August 2018; Received in revised form 12 March 2019; Accepted 14 March 2019
0168-1699/ © 2019 Elsevier B.V. All rights reserved.

Table 1
Comparison of field and laboratory methods for determining the effectiveness of kernel processing of whole plant corn silage.

KPS Assessment Method	Silage cup	Shaker box	Mechanical sieving	Image processing
Field or laboratory method	field	field	laboratory	field
Accuracy	low	variable based on shaking distance and speed and sample moisture content	industry standard	high
Quality metric	number of unbroken kernels	peNDF[a], WPCS[b] particle distribution	KPS[c], kernel particle size distribution	KPS
Preprocessing needed	no	no, if dry matter content higher than 45%	drying, kernel separation	kernel separation from WPCS
Preprocessing time	NA	hours, if drying needed	days for shipping, hours for drying	minutes
Quality metric estimation time	minutes	minutes	minutes	minutes

[a] Physically effective neutral detergent fiber.
[b] Whole plant corn silage.
[c] Kernel processing score.

a third screen to be added with an opening of 1.18 mm and defined a specific shaking frequency and amplitude to better describe the particle size distribution of WPCS for dairy cows and estimate the physically effective fiber. The shaker box method for assessing the particle size distribution of WPCS is more convenient for in-field measurements but requires measurement of the mass of material retained by each screen. Additionally, KPS could be determined via the shaker box method by pre-processing the sample. Pre-processing would include hydrodynamic separation of the corn kernels from the stover (Savoie et al., 2004) followed by drying of the corn kernels (ASABE, 2017). Shortcomings of this method include the potential for increased error due to the small number of sample points. A method for determining particle size distribution of WPCS during harvest, without the need to weigh samples, could increase the speed of assessment. Additionally, this method must allow for producers to accurately assess kernel processing to ensure it is sufficient for maintaining feed quality, ideally using the widely accepted KPS.

Image processing techniques have been used in the past to quantify particle size distributions of agricultural products. An image analysis plugin has been developed, capable of identifying particles in an image and defining their major orthogonal dimensions (Igathinathane et al., 2009b). The plugin successfully identified the shape of food grain and ground biomass and generated particle size distribution results with a mean absolute deviation of less than 1.2% for all shapes; however, these results were not compared to the standard method of sieving. Sieveless particle size distribution analysis has also been conducted using computer vision on several particulate materials (basmati rice, wheat straw, switchgrass, etc.) using open source ImageJ software (Igathinathane et al., 2009a; Igathinathane et al., 2009b). Particle size distribution determined via mechanical sieving of these materials showed that length-based inconsistencies are present when determining the particle size distribution of a sample especially for samples with a length much greater than the width however, these can be eliminated through the use of computer vision based size determination (Igathinathane et al., 2009a). Combining image analysis and mechanical sieving of chopped forages was found to provide a more complete estimation of mass and dimensional parameters of the chopped forages at theoretical length of cuts of 4.8, 9.5, and 11.1 mm (Savoie et al., 2014). Mechanical sieving is shown to underestimate particle length by 31% compared to image analysis. With the prevalence of smart devices and cameras in contemporary society, image analysis lends itself to the determination of particle size distribution. Correlations between sieve-based and image-based analysis of particles would allow for more rapid determination of sieve-based metrics such as KPS.

Image analysis has been used to assess particle size distribution in other research fields as well. Coarse aggregate particle size distribution was determined by image processing techniques for formulation of concrete mixtures (Mora et al., 1998). Results show that image analysis can successfully define course aggregate particle size, but limitations such as measurement resolution of the camera and the inability to compare directly to sieve results were cited. An autocorrelation algorithm was able to estimate the average grain size and distribution of bed sediment in near real-time in the field (Rubin, 2004). A machine vision approach has also been applied to characterizing the size distribution of mineral particles using a volume based approach (Igathinathane et al., 2012). A method to correlate image analysis results with sieve analysis results for particle size distribution determination of aggregates has also been developed (Fernlund et al., 2007). A minimum bounding square was defined for each aggregate in the image, which determined the minimum sieve size each particle would pass through. However, this analysis assumed a uniform density of material which may not be an appropriate assumption for agricultural materials. Techniques used in the characterization of aggregates could be applied to more uniform agricultural materials, such as corn kernels, to achieve accurate estimations of particle size while also correlating to the standard method of mechanical sieving. Allowing producers to accurately assess key particle size characteristics, would allow for the adjustment of crop processing rollers in-field during harvest to improve feed quality.

The impact of kernel particle size, as measured by KPS, at harvest to feed quality is significant. Currently, visual or mass-based assessment of chopped and processed corn silage is the only method available to producers to quantify sufficient crop processing during harvest (Table 1). However, visual inspection can be subjective and is typically limited to identifying the number of unbroken kernels within a 1 L sample of chopped forage and is not a measure of the size distribution of the kernels present (Shinners & Holmes, 2013). In field, manual sieving can be carried out, using the method outlined by Kononoff et al. (2003) but great care must to taken to shake the boxes in the prescribed method and weight the mass of particles on each sieve. While this method provides measurable data it does not provide an estimate of KPS without separating and drying the sample which would add a considerable amount of time to the process. To accurately quantify the distribution and estimate KPS, producers must send samples to a laboratory for mechanical sieving analysis, the standard method, resulting in turnaround times on the order of several days, well after the harvest is complete. Thus, a method that would allow for quantification of particle size distribution and estimation of KPS that could be completed on the order of minutes or hours would provide actionable, quantitative data to producers during harvest.

Specific objectives of this research were as follows: (1) Develop a robust image-processing algorithm for determination of particle size distribution of corn kernels in WPCS in the field during harvest (2) Compare the image analysis results to particles of a known size to determine algorithm accuracy and (3) Assess the image analysis results to determine if image processing can be an in-field alternative to sieved-based measurements of KPS.

2. Materials and methods

2.1. Sample collection

Chopped and processed whole-plant corn samples were collected in a production corn silage field at the University of Wisconsin-Madison Arlington Agricultural Research Station (Arlington, WI) in 2015 and 2016. A self-propelled forage harvester (SPFH) (940 Jaguar, Claas North America, Omaha, NE) equipped with an 8 row gather head and Shredlage™ crop processing rolls (Scherer Design Engineering Inc., Tea, SD) was used to harvest the standing corn. The theoretical length of cut was set to 19 mm during all data collection. The crop processor rolls were set at 1, 2, 3, and 4 mm roll gap clearances. At each roller clearance setting, standing corn was harvested and blown on the ground in piles for 15.24 m. Samples, approximately 600 mL per sample, of WPCS were pulled from each pile at random locations. Samples were placed in plastic sealable bags (Whirl-Pak 99100125, Nasco, Ft. Atkinson, WI) and were frozen within two hours of collection to maintain sample integrity and moisture content.

2.2. Image collection

2.2.1. Experimental apparatus

A simple lightbox was constructed to reduce the effect of shadows from overhead lighting and ensure consistent images throughout the experiment. An aluminum frame (80/20, T-slotted, 15 series) supported the camera (D7100, Nikon) and allowed for adjustment of the camera in the vertical (Y) and horizontal (Z) directions, Fig. 1. The floor of the lightbox was constructed of matte black poster board (902091, Elmer's Products, Inc., High Point, NC) to provide high contrast between the kernels. A white sheet was draped over the apparatus to diffuse light from three, 500 W halogen lights (GT-HL503, Smart Electrician). An aluminum calibration disc with an outside diameter of 38.1 mm, thickness of 3.175 mm, and center hole of 6.35 mm diameter was manufactured and used as a size reference within each image.

2.2.2. Verification images

Initial development of the image processing algorithm was undertaken using spherical pellets (ASP5020E, Crossman Corporation, Bloomfield, NY). The size of these calibration items was measured with digital calipers (500-321, Mitutoyo U.S.A., Aurora, IL) with a manufacturer stated accuracy of ± 0.025 mm. A random sample of 10 pellets was measured along three axes. Images were captured at three heights (0.4, 0.6, and 0.8 m) and five angles (0°, forward 10°, back 10°, left 10°, and right 10°). The 50 pellets were affixed to black paper to ensure they did not move while images were collected.

2.2.3. Kernel images

Each sample of WPCS (approximately 600 mL) was prepared by hydrodynamic separation of corn kernels and stover (Savoie et al., 2004; Shinners & Holmes, 2013), drying of the kernel portion of the sample (ASABE, 2017), and sieving of the kernel portion of the sample (ASABE, 2012). Images of samples were captured after thawing and hydrodynamic separation (wet), after drying at 55 °C for 72 h (dry), and after mechanical sieving as described in Section 2.1 (sieved). Each sample of corn kernels was divided into 1–3 g subsamples, resulting in 15–30 images per sample. Effort was taken to ensure that particles were not touching and were in a single layer approximately 0.2 by 0.3 m rectangle to fill the camera view window. A soft bristled brush was used to spread samples for imaging and to transfer samples to and from the storage container to minimize breaking of kernels. Images were captured at a height of 0.4 m with the camera lens perpendicular to the image background.

2.3. Algorithm development

The determination of KPS using the proposed image processing method consists of sample collection, sample preprocessing, sample imaging, and image analysis (Fig. 2). Analysis of individual images was done utilizing MATLAB Software (Mathworks, 2016) and its included Image Processing Toolbox. The developed algorithm completes preprocessing of the image, identifies kernels within the image, measures the diameter and cross sectional area of the identified particles, and computes relevant statistics of the kernel size distribution.

Once the image was loaded into the software it was converted to gray scale and then denoised using total variation denoising (Rudin et al., 1992) This denoising method is widely used in state-of-the-art image processing pipelines and is particularly well-suited to images with large regions with almost constant brightness, such as in our setting. The largest diameter circular region in the image (calibration disk described in Section 2.2.1) was identified using the circle Hough transform (CHT) (Hough, 1959, 1962; Mathworks, 2016). The CHT is based on the fact that any circle can be described by its radius (r) and center, and that if we place a new circle of radius 2r at each point on the perimeter of the original circle, they will all intersect at the center of the original circle. This geometric insight leads to a re-parameterization of the image data so that peaks in the reparametrized image immediately tell us the location and sizes of circles in the original image. The largest circular region corresponds to our landmark coin or washer and lets us automatically calibrate our algorithm by determining the pixel to mm scale for each image. Next we must separate the kernel particles from the image background. A naïve approach involved simply looking for connected sets of pixels above a certain brightness level. However, we found that this approach was (a) sensitive to variable and unpredictable lighting conditions and (b) sensitive to noisy or pixel variability that persisted even after the image denoising step described above. To sidestep these challenges, we extracted Maximally Stable External Regions (MSER) to separate kernel from the dark background (Matas et al., 2004) MSER thresholds an image at a variety of brightness levels, and selects sets of pixels which form a contiguous region whose size changes minimally as the threshold level varies. These sets of pixels correspond to our extracted kernel pieces; by looking at a variety of

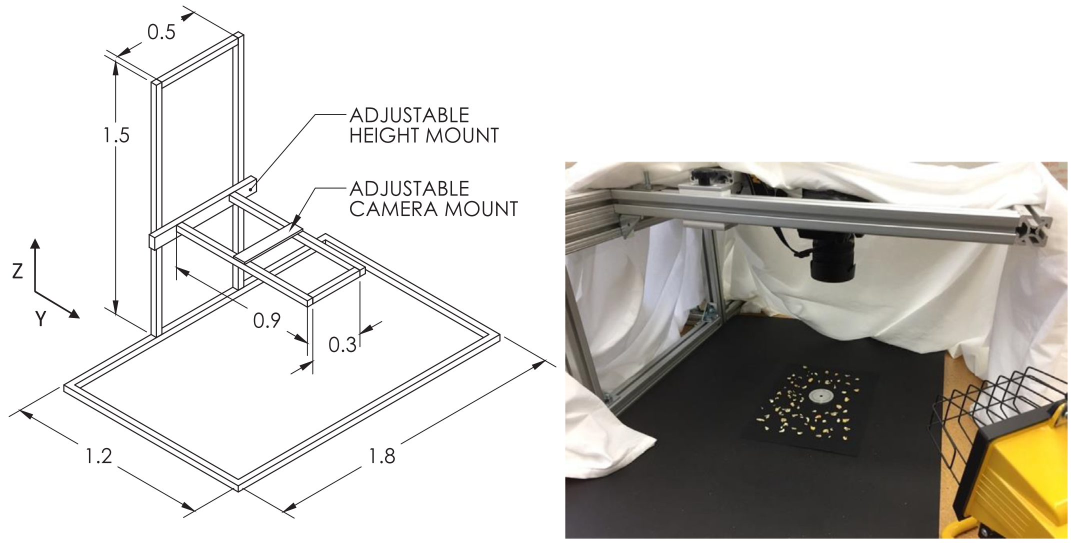

Fig. 1. Schematic of the lightbox for sample imaging, all dimensions in meters.

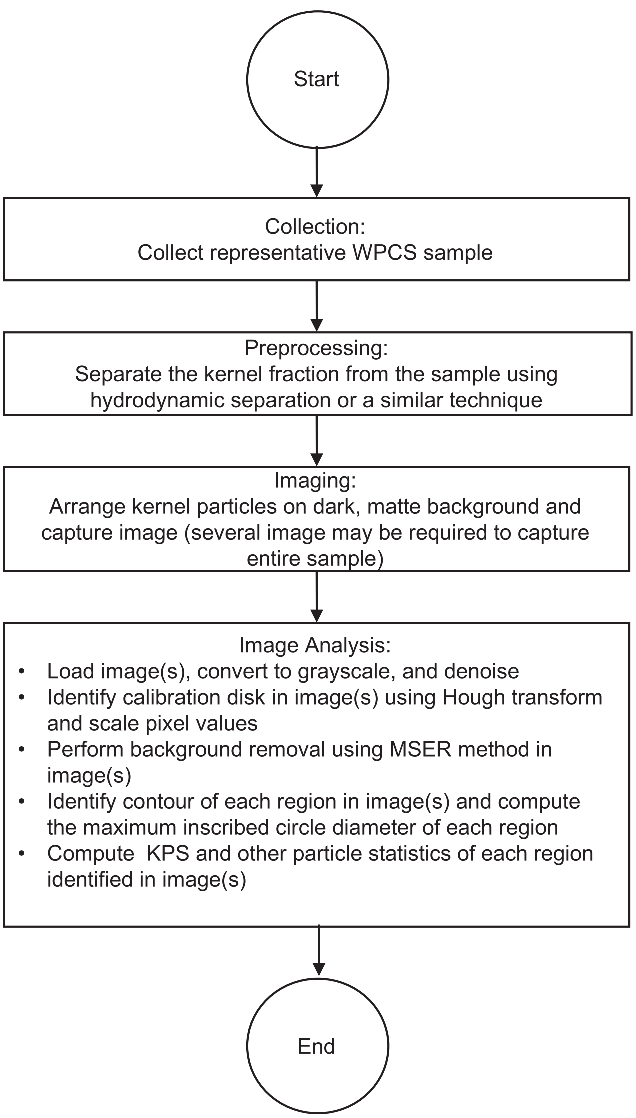

Fig. 2. Flow diagram of sample collection, preprocessing, image analysis and Kernel Processing Score (KPS) determination of whole plant corn silage (WPCS) samples using the proposed algorithm.

brightness thresholds this way, MSER achieves a desirable robustness to lighting conditions and noise. We then extracted the boundaries of these regions to define the kernel contours and used them to compute the cross-sectional area of each kernel. Then, the maximum inscribed circle diameter of each contour was determined (Birdal, 2011). We focus on the maximum inscribed circle because this is closely related to whether a kernel particle will fit through a sieve of a given size. The contour area and diameter were then scaled based on the known diameter of the calibration disk.

The percent undersize of particles and their corresponding dimensions of significance were calculated for each sample using mass weighting for sieve analysis and cross-sectional area weighting for image analysis (ASABE, 2012). Kernel Possessing Score (KPS) was derived from the area-weighted cumulative undersize percent of 4.75 mm. In addition, particle size distribution parameters including the graphic mean, inclusive graphic standard deviation, inclusive graphic skewness, and graphic kurtosis were calculated (Blott & Pye, 2001; Folk and Ward, 1957; Igathinathane et al., 2009b):

$$X_g = \frac{D_{16} + D_{50} + D_{84}}{3} \tag{1}$$

$$\sigma_{ig} = \left[\frac{D_{84} - D_{16}}{4}\right] + \left[\frac{D_{95} - D_5}{6.6}\right] \tag{2}$$

$$S_{ig} = \left[\frac{D_{84} + D_{16} - 2D_{50}}{2(D_{84} - D_{16})}\right] + \left[\frac{D_{95} + D_5 - 2D_{50}}{2(D_{95} - D_5)}\right] \tag{3}$$

$$K_g = \left[\frac{D_{95} - D_5}{2.44(D_{75} - D_{25})}\right] \tag{4}$$

where X_g is the graphic mean (mm), σ_{ig} is the inclusive graphic standard deviation (mm), S_{ig} is the inclusive graphic skewness (dimensionless), and K_g is the graphic kurtosis (dimensionless), and D is the corresponding particle lengths of the cumulative undersize percent identified by the subscript (mm). For image analysis, the geometric mean particle size was calculated using the maximum inscribed circle diameter. For sieve analysis the geometric mean particle size was calculated according to ASABE Standard S319.4 (ASABE, 2012):

$$d_{gw} = \log^{-1}\left[\frac{\sum_{i=1}^{n} W_i \log \bar{d}_i}{\sum_{i=1}^{n} W_i}\right] \tag{5}$$

Where n is the number of sieves and pan, W_i is the mass of material on the ith sieve (g), and $\bar{d}_i$ is the square root of the product of the nominal sieve aperture for the i and i + 1 sieve (mm).

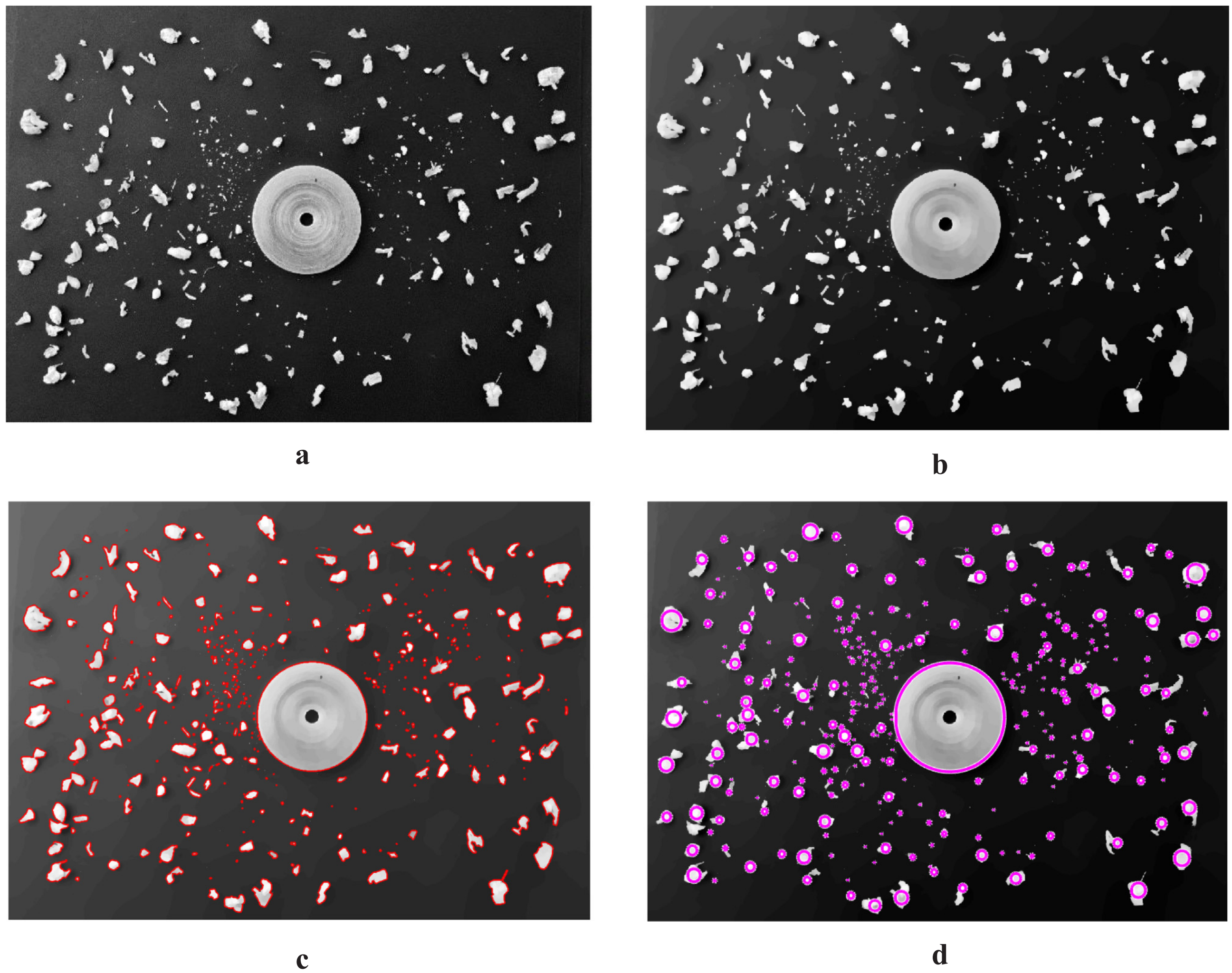

Fig. 3. Example of the steps of the image processing algorithm (a) image is imported, (b) image was denoised, (c) contour of each particle was identified, (d) maximum inscribed circle of each particle was identified.

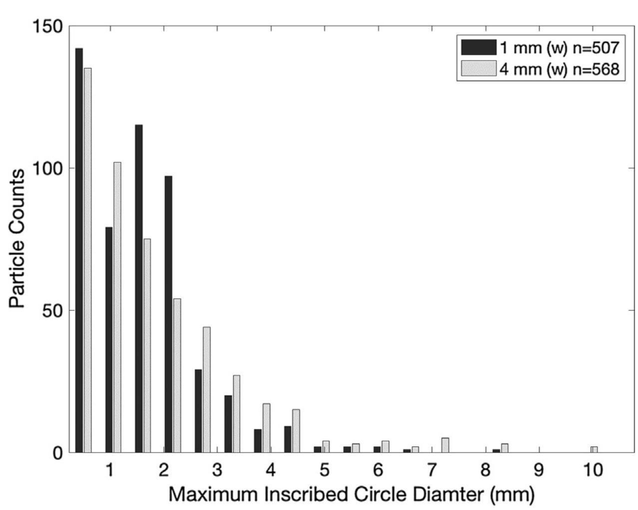

Fig. 4. Example of normalized histogram of the distribution of particle diameter for wet (w) samples processed with 1 and 4 mm kernel processer roll gap sizes, n is the number of particles within the image.

2.4. Seive analysis

Samples were dried in a non-hygroscopic container at 55 °C for 72 h to preserve the potential for future chemical analysis (ASABE, 2017). Dried samples were mechanically separated (RoTap R-29, W.S. Tyler) with sieves of ISO size 9.5, 6.3, 4.75, 3.35, 2.36, 1.7 1.18, 0.85, 0.6, and 0.425 mm. The sieve was operated for 15 min for each sample (ASABE, 2012). The mass of sample on each tray was measured and recorded (OPH-P, Optima Scale Manufacturing, Inc.) with special care taken to ensure all particles were removed from sieve trays due to the low sample volume. Samples were weighed before and after to ensure no more than 1% change in mass during analysis. The mass of particles on each sieve were used to calculate the geometric mean particle diameter and cumulative percent of particles smaller than each sieve diameter in accordance with ANSI/ASE S319.4 (ASABE, 2012)

2.5. Statistical analysis

A one sample *t*-test was used to compare the estimated mean spherical pellet diameter with the measured mean diameter for image processing model validation purposes. Statistical analysis of KPS as a function of crop processing roll gap clearance, for samples in each state, was conducted using the MIXED Procedure in SAS and means were separated using Tukey's method (SAS, 2013). Interactions effects were partitioned using the SLICE option (SAS, 2013). The KPS data were

Table 2
Percent undersize of 4.75 mm (Kernel Processing Score) by area (image analysis) or by mass (sieve analysis).

Processing Roll Gap (mm)	Year	Image analysis (by area)						Sieve analysis (by weight)	
		wet sample		dry sample		sieved sample			
		mean	SD	mean	SD	mean	SD	mean	SD
1	2015	75.0	2.1	85.9	3.7	88.6	2.7	83.9	2.9
2	2015	75.0	2.5	84.7	4.1	86.7	2.4	81.4	7.0
3	2015	69.7	5.3	84.3	3.0	88.2	0.7	79.2	3.0
4	2015	76.9	3.7	86.3	2.2	86.5	2.5	79.0	6.5
1	2016	75.7	5.4	83.4	3.0	85.1	2.3	80.3	4.1
2	2016	71.3	2.2	81.2	2.8	82.3	3.2	75.0	6.4
3	2016	70.3	1.3	79.6	0.8	81.2	0.5	77.1	2.1
4	2016	60.5	3.8	73.6	2.4	75.2	1.3	63.0	2.1

Table 3
P-values of paired *t*-test of percent undersize, by image processing, for samples before and after mechanical sieving. Bold values are significantly different under alpha = 0.05. Percent undersize of 4.75 mm is equivalent to kernel processing score.

Processing roll gap (mm)	Area weighted cumulative percent of particles smaller than (mm)								
	6.3	4.75	3.35	2.36	1.7	1.18	0.85	0.6	0.43
1	**0.01**	**0.00**	**0.04**	0.07	**0.04**	**0.02**	**0.03**	**0.04**	0.24
2	0.06	**0.01**	**0.00**	**0.04**	0.06	0.08	0.06	0.06	0.35
3	**0.04**	**0.02**	**0.03**	0.07	0.07	0.17	0.14	0.28	0.33
4	**0.03**	0.41	1.00	0.79	0.64	0.66	0.81	0.97	0.74

Table 4
Mean Kernel Processing Score by crop processing roll gap for by image analysis for wet samples under alpha = 0.05. Means with different letters are significantly different.

Processing Roll Gap (mm)	Year	Estimate	Standard Error	Letter Group
4	2015	76.9	1.8	A
1	2016	75.8	2.1	A
1	2015	75.0	2.1	A
2	2015	75.0	2.1	A
2	2016	71.3	2.1	A
3	2016	70.3	2.1	AB
3	2015	69.7	2.1	AB
4	2016	60.5	2.1	B

Table 5
Percent undersize of 2 mm by crop processing roll gap for by image analysis for wet samples under alpha = 0.05. Means with different letters are significantly different.

Processing Roll Gap (mm)	Year	Estimate	Standard Error	Letter Group
1	2015	39.4	2.3	A
4	2015	38.2	2.0	A
2	2015	33.5	2.3	AB
1	2016	30.4	2.3	AB
3	2015	26.5	2.3	BC
2	2016	26.2	2.3	BC
3	2016	26.2	2.3	BC
4	2016	18.6	2.3	C

assessed for the assumption of normality of residuals and constant variance using graphical methods. Paired *t*-test were used to compare means of KPS using image processing techniques before and after mechanical sieving. A Bland-Altman plot was used to assess the agreement between image processing and sieving methods to determine KPS.

3. Results

3.1. Image analysis

Images of 1, 2, 3, and 4 mm samples collected in 2015 and 2016 were processed using the developed algorithm. Each sample was divided into 10–20 subsamples for imaging to facilitate the arrangement of particles in a single layer without overlap. Results of each image were inspected visually to ensure all kernels fell within the view window and were not overlapping. An example of the steps of the algorithm for a single subsample can be seen in Fig. 3. A normalized histogram of the distribution of particle diameters within 1 mm and 4 mm samples of wet kernels highlights the differences in distribution patterns with the 4 mm sample skewed toward larger particle diameters (Fig. 4).

KPS was determined by image (for wet, dry, and sieved samples) and sieve analysis (measured between dry and sieved images) for 28 samples and the results summarized (Table 2). KPS increased after drying as expected because the drying processes reduced the size of particles and reduced clumping of multiple particles. The increase in KPS after mechanical sieving indicated that the sieving process reduced the size of kernel particles.

Two sample *t*-test of the cumulative undersize percent, by area, for each sieve size for dry and sieved samples were conducted to quantify the effect of sieving on particle size (Table 3). The decrease in particle size after sieving was more prevalent in the cumulative undersize percent of particles for the largest sieve sizes.

Mean KPS, determined by image analysis of wet samples, was significant by processor gap size ($P = 0.017$), sample year ($P = 0.004$), and their interaction ($P = 0.0012$) (see Table 4). Analysis of the simple effects found gap size to be significant for only the 2016 data ($P = 0.0006$). Means were separated by gaps size and year using Tukey's Method (Table 3). Percent undersize of 2 mm particles was also assessed (Table 5) and found to be significant by gap ($P = 0.01$), year ($P < 0.0001$), and their interaction ($P = 0.0038$). Chemical analysis of samples, pooled by gap size and year, was conducted to ensure no anomalies were present in the concentration of crude protein, fiber and starch (Rock River Laboratories, Watertown, WI). Values, as a percent

Table 6
Geometric mean particle size, by image analysis of wet samples and sieve analysis of dry samples.

Processing Roll Gap (mm)	Year	Image analysis (by area)						Sieve analysis (by weight)	
		Graphic mean X_g (mm)	Graphic SD σ_{ig} (mm)	Skewness S_{ig}	SD	Kurtosis K_g	SD	Geometric Mean Diameter d_{gw} (mm)	SD (mm)
1	2015	2.5	1.6	0.61	0.07	1.2	0.3	2.5	2.2
2	2015	2.7	1.3	0.37	0.22	1.0	0.3	2.6	2.2
3	2015	3.3	1.7	0.21	0.13	0.9	0.1	2.8	2.2
4	2015	2.9	1.6	0.38	0.24	1.1	0.4	2.6	2.3
1	2016	3.7	1.9	0.26	0.08	0.9	0.1	2.6	2.0
2	2016	3.6	1.7	0.22	0.07	0.8	0.1	2.8	2.1
3	2016	3.7	2.0	0.24	0.03	0.9	0.1	2.8	2.0
4	2016	4.4	2.3	0.24	0.09	0.8	0.1	3.3	2.5

Table 7
Mean Kernel Processing Score by crop processing roll gap for by sieve analysis under alpha = 0.05. Means with different letters are significantly different.

Processing Roll Gap (mm)	Estimate	Standard Error	Letter Group
1	82.6	1.9	A
2	78.2	2.0	AB
3	78.2	2.2	AB
4	71.6	2.0	B

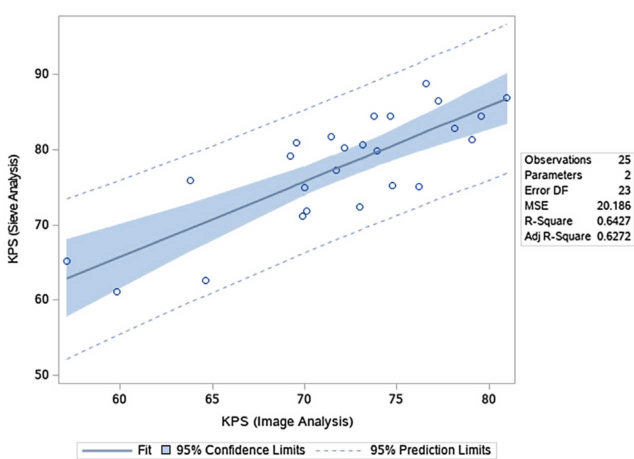

Fig. 5. Sieve analysis of dry sample vs image analysis of wet sample of Kernel Processing Score.

of dry matter were consistent across gap size and year for protein (M = 8.61, SD = 0.32), starch (M = 73.4, SD = 1.0), and fiber (M = 3.37, SD = 0.43).

The graphic mean, inclusive graphic standard deviation, inclusive graphic skewness, and graphic kurtosis were calculated using image analysis results using Eqs. (1)–(4) (Table 6). The geometric mean diameter (Eq. (5)) was calculated from sieve analysis results (Table 6). Image analysis tended to estimate larger particle size than sieve analysis. Particle distributions were fine (0.1–0.3) to very fine (0.3–1.0) skewed. Most distributions were classified as mesokurtic, having the same kurtosis as a normal distribution.

3.2. Seive analysis

All samples were sieved between capturing dry and sieved images. Mean KPS, determined by sieve analysis, was significant by gap size ($p = 0.0078$) and sample year ($p = 0.0023$). Means were separated by gap size and year using Tukey's Method (Table 7). The results were similar to those of the image analysis method. KPS was estimated as 80.9 (S.E. = 1.4) for 2015 and 73.9 (S.E. = 1.3) for 2016.

3.3. Algorithm verification

3.3.1. Anaysis of paticles of known diamter

The one sample *t* test failed to reject the hypothesis that the estimated mean spherical pellet diameter (at a height of 0.4 m and no angle) came from the same distribution as the measured spherical pellet diameter of 5.97 mm ($P = 0.27$). The height at which the image was captured was found to be significant ($P < 0.0001$). The pairwise comparison of means using Tukey's method found that the mean at all heights were significantly different from each other with the estimated particle diameter found to be 6.01 mm (SE 0.03), 5.62 mm (SE 0.03), and 5.19 mm (SE 0.03) for images taken at a height of 0.4, 0.6, and 0.8 m, respectively. The image processing algorithm was able to accurately (less than one percent difference between estimated and actual particle diameter) predict particle size for heights less than 0.4 m and all subsequent images were captured at this height.

3.3.2. Comparison of image and sieve analysis

A significant ($P < 0.0001$) correlation between image based (wet sample) and sieve based KPS was found with a Pearson correlation coefficient of $r(23) = 0.8$. The relationship between image and sieve analysis can be described by Eq. (5). Wet samples were used as the basis for image analysis comparison as this will be expected use for determining KPS in the field during harvest (Fig. 5).

$$KPS_{sieve} = 5.76 + KPS_{image} \quad (6)$$

A Bland Altman analysis was also performed to assess the agreement of sieve and image processing results over the range of KPS values (see Fig. 6). The difference between methods was consistent across the range of KPS and for all gap sizes with mean difference of 5.8. The lowest difference between sieve and image analysis was seen for 4 mm samples.

4. Discussion

4.1. Image analysis

Image based characterization of particle distribution of corn kernels processed through 1, 2, 3, and 4 mm processer gap found a trend of decreasing KPS with increasing gap size with significant differences between 4 mm and 1, 2, and 3 mm gaps sizes. However, inconsistencies within the trends suggests that regular monitoring of KPS between years and fields is critical in maintaining feed quality. These finding were consistent with studies finding increased total tract starch digestibility with whole plant corn silage processes using 1–3 mm gap settings as compared with 4–8 mm gap settings (Ferraretto & Shaver, 2012). Diets containing high moisture corn with a mean particles size of less than 2 mm have been shown to have increased starch digestibility (Ferraretto et al., 2013). However, estimates of mean particle diameter by both sieve and image analysis were found to be greater than 2 mm but the percent undersize of 2 mm particles were significantly different by gap size. Changes in processing could lead to increases in more

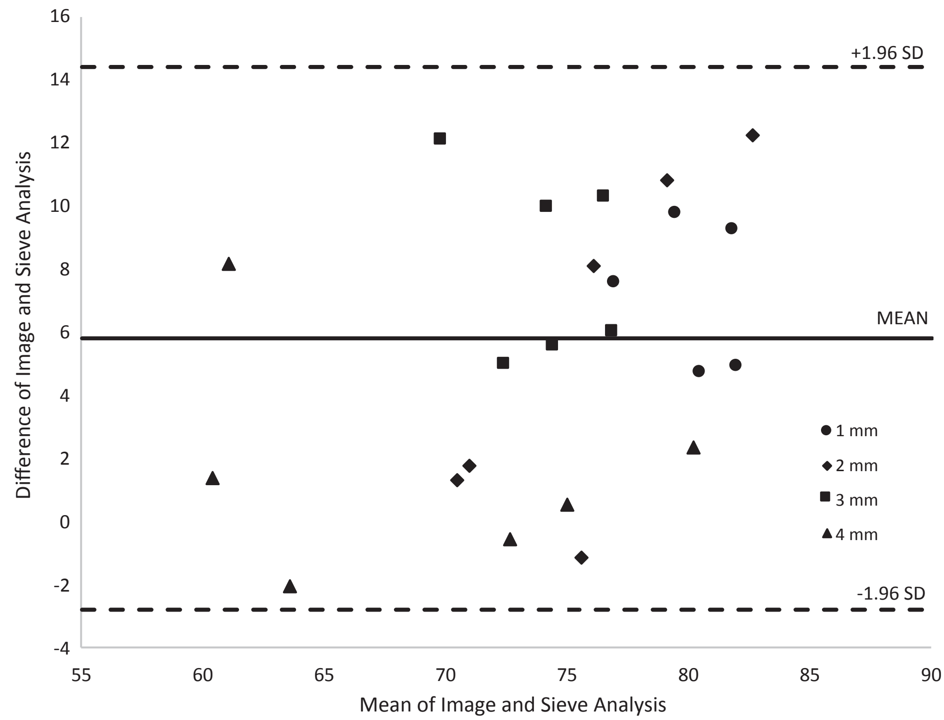

Fig. 6. Bland-Altman plot of sieve and image analysis results for Kernel Processing Score.

readily digestible particles but can be a function of year.

4.2. Sieve analysis

Sieve analysis of KPS had similar trends to those found using image analysis with 1 mm gap size having a significantly higher KPS than 4 mm gap size. The data suggest that mechanically sieving changes the particle size distribution of kernel particles. The decrease in particle size after sieving was more prevalent in the cumulative undersize percent of particles for the largest sieve sizes indicating that large particles were more likely to be damaged during the sieving process. The lack of a significant difference of the 4 mm gap sample for most sieve sizes, may be due to these samples containing the highest number of uncracked kernels which would most likely not be affected by sieving.

4.3. Algorithm verification

The image processing algorithm was able to accurately predict mean particle diameter of particles of a known size. The height of the camera was found to affect the accuracy of prediction as the number of pixels per particle decreases. KPS estimated by sieve and image analysis were well correlated. The differences between the methods are most likely due to differences in density within the kernel and varying thickness of each particle. Fernlund et al. (2007) also found a good correlation between sieve and image analysis using a similar technique, the minimum bounding square, for aggregate particles. Additionally, the discrepancies would arise from the “width-based separation” of particles during mechanical sieving. Igathinathane et al. (2009b) found that the effect of particles “falling through” the sieves to underestimate the length of particles by approximately a factor of 20. While the ratio of length to width of kernel particles is not as large as the biomass analyzed by Igathinathane et al. (2009b), differences in length to with ratio can bias sieve based particle size measurements.

4.4. In-field application

The image analysis method developed and described in this manuscript was intended to provide an estimate of KPS in field, in a time frame that would allow for adjustment during harvesting. WPCS samples must be collected in the field or at the storage site. First, hydrodynamic separation can be used to remove the stover from the sample and can be completed in less than 30 min. Then samples are imaged against a dark background. Depending on the level of detail given to separating the kernel particles, a sample can be imaged in 30 min to 2 h, assuming 20 image per sample and 1–5 min per image. Finally, the images must be analyzed via the developed algorithm which takes approximately 30 min to 1 h and can be done concurrently with imaging, assuming 20 image per sample and 1–3 min per image. This process can be carried out with a dishpan, black matte surface, camera, a computer, and access to water. KPS can be determined in a few hours as compared to days when sending a sample to the laboratory.

5. Conclusions

Image processing techniques were found to effectively predict the KPS as compared to the standard method of mechanical sieving. Algorithm results were compared with the standard method of drying and sieving and found to be well correlated $r(23) = 0.8$, $p < 0.001$ and Bland-Altman plots demonstrated the difference in predicted KPS to be consisted over the range of KPS explored. Mechanical sieving was also found to reduce particles size and increase the KPS for 1, 2, and 3 mm gap sizes which may bias laboratory results.

This image processing method can decrease the time to determine KPS, as compared with standard laboratory methods, and allow for adjustment of kernel processing rolls during harvest. Sample collection, preprocessing, imaging, and determination of KPS can be completed on the order of hours, as compared to a turnaround time of days with the standard laboratory sieve method. Additionally, this work has implications into the proper level of kernel processing and future work should focus on assessing different machines and kernel processors.

Acknowledgements

Funding for this research was provided by the Midwest Forage Association's Midwest Forage Research Program.

References

ASABE, 2012. Method of Determining and Expressing Fineness of Feed Materials by Sieving (ANSI/ASAE S319.4). Retrieved from https://www.asabe.org/.
ASABE, 2017. Moisture Measurement- Forages (ANSI/ASAE S358.3). Retrieved from https://www.asabe.org/.
Birdal, T., 2011. Maximum Inscribed Circle using Distance Transform. Retrieved from https://www.mathworks.com/matlabcentral/fileexchange/30805-maximum-inscribed-circle-using-distance-transform (accessed 09.03.19).
Blott, S.J., Pye, K., 2001. GRADISTAT: a grain size distribution and statistics package for the analysis of unconsolidated sediments. Earth Surf. Proc. Land. 26 (11), 1237–1248. https://doi.org/10.1002/esp.261.
Fernlund, J.M.R., Zimmerman, R.W., Kragic, D., 2007. Influence of volume/mass on grain-size curves and conversion of image-analysis size to sieve size. Eng. Geol. 90 (3–4), 124–137. https://doi.org/10.1016/j.enggeo.2006.12.007.
Ferraretto, L.F., Crump, P.M., Shaver, R.D., 2013. Effect of cereal grain type and corn grain harvesting and processing methods on intake, digestion, and milk production by dairy cows through a meta-analysis. J. Dairy Sci. 96 (1), 533–550. https://doi.org/10.3168/jds.2012-5932.
Ferraretto, L.F., Shaver, R.D., 2012. Meta-analysis: Effect of corn silage harvest practices on intake, digestion, and milk production by dairy cows. Professional Animal Sci. 28 (2), 141–149. https://dx.doi.org/10.15232/S1080-7446(15)30334-X.
Folk, R.L., Ward, W.C., 1957. Brazos River bar: a study in the significance of grain size parameters. J. Sediment. Res. 27 (1).
Hough, P.V.C., 1959. Machine analysis of bubble chamber pictures. In: Proc. Int. Conf. on High Energy Accelerators and Instrumentation. CERN, Geneva, Switzerland, pp. 554–558.
Hough, P.V.C., 1962. Method and Means for Recognizing Complex Patterns. USA Patent No. 3,069,654.
Igathinathane, C., Pordesimo, L.O., Batchelor, W.D., 2009a. Major orthogonal dimensions measurement of food grains by machine vision using ImageJ. Food Res. Int. 42 (1), 76–84. https://doi.org/10.1016/j.foodres.2008.08.013.
Igathinathane, C., Pordesimo, L.O., Columbus, E.P., Batchelor, W.D., Sokhansanj, S., 2009b. Sieveless particle size distribution analysis of particulate materials through computer vision. Comput. Electron. Agric. 66 (2), 147–158. https://doi.org/10.1016/j.compag.2009.01.005.
Igathinathane, C., Ulusoy, U., Pordesimo, L.O., 2012. Comparison of particle size distribution of celestite mineral by machine vision ΣVolume approach and mechanical sieving. Powder Technol. 215, 137–146. https://doi.org/10.1016/j.powtec.2011.09.037.
Johnson, L.M., Harrison, J.H., Davidson, D., Mahanna, W.C., Shinners, K.J., 2003. Corn silage management: Effects of hybrid, chop length, and mechanical processing on digestion and energy content. J. Dairy Sci. 86 (1), 208–231. https://doi.org/10.3168/jds.S0022-0302(03)73601-7.
Kononoff, P.J., Heinrichs, A.J., Buckmaster, D.R., 2003. Modification of the Penn State forage and total mixed ration particle separator and the effects of moisture content on its measurements. J. Dairy Sci. 86 (5), 1858–1863. https://doi.org/10.3168/jds.S0022-0302(03)73773-4.
Lammers, B.P., Buckmaster, D.R., Heinrichs, A.J., 1996. A simple method for the analysis of particle sizes of forage and total mixed rations. J. Dairy Sci. 79 (5), 922–928. https://doi.org/10.3168/jds.S0022-0302(96)76442-1.
Matas, J., Chum, O., Urban, M., Pajdla, T., 2004. Robust wide-baseline stereo from maximally stable extremal regions. Image Vis. Comput. 22 (10), 761–767. https://doi.org/10.1016/j.imavis.2004.02.006.
Mathworks, 2016. Matlab Help and Documentation (Version r2016a). Mathworks, Cambridge, MA (accessed 09.03.19).
Mertens, D.R., 2005. Particle size, fragmentation index, and effective fiber: Tools for evaluating the physical attributes of corn silages. In: 4-State Dairy Nutrition and Management Conference. Midwest Plan Service, Iowa State Univ, Ames, Iowa, pp. 211–220.
Mora, C.F., Kwan, A.K.H., Chan, H.C., 1998. Particle size distribution analysis of coarse aggregate using digital image processing. Cem. Concr. Res. 28 (6), 921–932. https://doi.org/10.1016/S0008-8846(98)00043-X.
Rubin, D.M., 2004. A simple autocorrelation algorithm for determining grain size from digital images of sediment. J. Sediment. Res. 74 (1), 160–165. https://doi.org/10.1306/052203740160.
Rudin, L.I., Osher, S., Fatemi, E., 1992. Nonlinear total variation based noise removal algorithms. Phys. D: Nonlinear Phenomena 60 (1–4), 259–268. https://doi.org/10.1016/0167-2789(92)90242-F.
SAS, 2013. SAS 9.4 Help and Documentation (Version 9.4). SAS Institute, Inc., Cary, NC (accessed 09.03.19).
Savoie, P., Audy-Dube, M.A., Pilon, G., Morissette, R., 2014. Length distribution and other dimensional parameters of chopped forage by image analysis. Trans. Asabe 57 (6), 1549–1555. https://dx.doi.org/10.13031/trans.57.10665.
Savoie, P., Shinners, K.J., Binversie, B.N., 2004. Hydrodynamic separation of grain and stover components in corn silage. Appl. Biochem. Biotechnol. 113 (1), 41–54. https://doi.org/10.1385/abab:113:1-3:041.
Shinners, K.J., Holmes, B.J., 2013. Making sure your kernel processor is doing its job. Retrieved from. Focus Forage 15 (4), 1–3. http://fyi.uwex.edu/forage/files/2014/01/KernelProcessing-FOF.pdf.
Shinners, K.J., Jirovec, A.G., Shaver, R.D., Bal, M., 2000. Processing whole-plant corn silage with crop processing rolls on a pull-type forage harvester. Appl. Eng. Agric. 16 (4), 323–331. https://dx.doi.org/10.13031/2013.5214.
Weiss, W.P., Wyatt, D.J., 2000. Effect of oil content and kernel processing of corn silage on digestibility and milk production by dairy cows. J. Dairy Sci. 83 (2), 351–358. https://doi.org/10.3168/jds.S0022-0302(00)74886-7.